International Journal of Science and Research (IJSR)
ISSN (Online): 2319-7064
Index Copernicus Value (2015): 78.96 | Impact Factor (2015): 6.391

Vibrational Spectra (FT-IR, FT-Raman and NMR) of 1, 5-Difluoro-2,4-dinitrobenzene based on Density Functional Calculations

S. Seshadri[1], M. Padmavathy[2]

[1]PG & Research Department of Physics, Urumu Dhanalakshmi College, Kattur, Trichy-620019, India

[2]Department of physics, Shrimati Indira Gandhi College, Trichy-620002, India

Abstract: ***The experimental and theoretical study on the structures and vibrations of 1,5-Difluoro-2,4-dinitrobenzene (DFDNB) is analyzed. The Fourier transform infrared (FT-IR) spectrum (4000–400 cm^{-1}) and the Fourier transform Raman (FT-Raman) spectrum (3500–100 cm^{-1}) of the title molecule have been recorded. The complete assignments were performed on the basis of the potential energy distribution (PED) of the vibrational modes calculated with scaled quantum mechanical (SQM) method. The molecular structures and vibrational frequencies, infrared intensities and Raman scattering actives have been calculated. ^{13}C and ^{1}H NMR chemical shifts results were also compared with the experimental values.***

Keywords: FT-IR, FT-Raman, PED, SQM, NMR

1. Introduction

Nitrobenzene is an organic compound with the chemical formula C6H5NO2. It is water-insoluble pale yellow oil with an almond-like odor. It freezes to give greenish yellow crystals. It is produced on a large scale as a precursor to aniline. Although occasionally used as a flavoring or perfume additive, nitrobenzene is highly toxic in large quantities. In the laboratory, it is occasionally used as a solvent, especially for electrophilic reagents. Aromatic compound such as benzene derivative of fluoronitrobenzene is commonly used in pharmaceutical products. Benzene under goes nitration and halogenations, then the reactions of the benzene slow down. Nitrofluorobenzene are produced for industrial uses such as dyes, drugs, pesticides, shoe polish, spray paint, and synthetic rubber [1,2].

Fluorine substituent can greatly increase the fat solubility of molecules, which is particularly important in pharmaceuticals where it can increase their bioavailability. Molecules including more fluorine, amplifies the effect and have regular feature in both drug and agrochemical actives. Numerous common fungicides also contain fluorine atoms. Fluorine is a common element in antibiotic molecules, too. Fluorine has become a popular feature in drugs and agrochemicals because of the effects it exerts in molecules. The anti-inflammatory drugs are designed to treat rheumatoid arthritis [1].

Fluorine is the most electronegative atom of all the compounds. It pulls electrons toward it, thus reducing the electron density at the carbon in a C–F bond. It also affects the molecule's dipole moment and the molecule's over all stability. Nitrobenzene is an aromatic nitro compound. Most nitrobenzene (97%) is used in the manufacturing of aniline. Nitrobenzene is highly toxic in large quantities and is mainly produced as a precursor to aniline. In the laboratory it finds occasional use as a solvent especially for electrophilic [2].

Nitrobenzene can cause a wide variety of harmful health effects to exposed persons. Repeated exposures to a high concentration of nitrobenzene can result in a blood condition called methemoglobinemia (a form of anemia). This condition affects the ability of blood carrying oxygen [3]. Exposure level is extremelyhigh nitrobenzene can cause coma and possibly death unless prompt medical treatment is received. In case of long-term exposure to nitrobenzene, the presence of its breakdown products, p-nitrophenol and p-aminophenol, in the urine is an indication of nitrobenzene exposure. The results of these tests cannot be used to determine the level of nitrobenzene exposure [4, 5].

Therefore the fluorine substituted nitrobenzene is also used to produce pharmaceutical drugs and agrochemical products. Various spectroscopic studies of halogen substituted compounds have been reported in the literature [6–8] so far. The molecular structure of ortho and para fluoronitrobenzene have been investigated by HF and DFT calculations [9]. However, no FT-IR, FT-Raman and NMR analysis of DFT calculation with B3LYP method at 6−31++G(d,p) basis set is reported on DFDNB so far, in spite of its pharmaceutical importance. Hence, in the present work a detailed DFT vibrational structure analysis has been attempted by recording FT-IR and FT-Raman spectra of the compound DFDNB considering its biological and pharmaceutical uses.

2. Experimental Details

The fine polycrystalline samples of a 1,5-Difluoro-2,4-dinitrobenzene (DFDNB) was used for the spectral measurements. Fourier transform infrared (FT-IR) spectra of the title compounds are recorded with KBr pellet technique in the 4000–400 cm^{-1} region using BRUKER IFS-66V FT-IR spectrometer equipped with a cooled MCT detector for the mid-IR range at room temperature. The FT-Raman spectra was recorded on a BRUKER IFS-66V model interferometer equipped with an FRA-106 FT-Raman accessory. The spectra were recorded in the 3000–100 cm^{-1}

stokes region using 1064 nm line of an Nd:YAG laser for excitation operating at 200 mW power. The reported frequencies were accurate, ±1 cm^{-1} for FT-IR and FT-Raman. ^{13}C and ^{1}H NMR spectra were taken in CDCl3 solutions and all signals were referenced to TMS on a BRUKER TPX-400 FT-NMR spectrometer.

3. Computational Details

The molecular geometry optimization and vibrational frequency calculations were carried out for DFDNB with Gaussian 09W software package [10] using the B3LYP functional [11, 12] with standard 6-311++G(d,p) basis set. The Cartesian representation of the theoretical force constants were computed at optimized geometry by assuming C1 point group symmetry. Scaling of the force field was performed according to the SQM procedure [13, 14] using selective scaling in the natural internal coordinate representation [15, 16]. Transformation of the force field and subsequent normal coordinate analysis including the least square refinement of the scale factors, calculation of the potential energy distribution (PED) and the prediction of IR and Raman intensities were done on a PC with the Molvib program (version 7.0-G77) by Sundius [17, 18]. For the graphs of simulated IR and Raman spectra, pure Lorentzian band shapes were used with a band width of 10 cm^{-1}.

The symmetry of the molecule was also helpful in making vibrational frequencies. The symmetries of the vibrational modes were determined using the standard procedure of transforming the traces of the symmetry operation into irreducible representation. The symmetry analysis for the vibrational modes of DFDNB was done in detail in order to describe the basis for the frequencies. By combining the results of the Gaussview program with symmetry considerations, vibrational frequency analysis was made with a high degree of accuracy. There was always some ambiguity in defining the internal coordinates. However, the defined coordinates form a complete set and match quite well with the motions observed using the Gauss view program.

The Raman activities (S_i) calculated by the Gaussian 09W program was converted to relative Raman intensities (I_i) using the following relationship derived from the intensity theory of Raman scattering [19, 20].

$$I_i = \frac{f(\nu_0 - \nu_i)^4 S_i}{\nu_i[1 - \exp(-hc\nu_i / KT)]} \quad (1)$$

where ν_0 is the laser exciting wavenumber in cm^{-1} (in this work, we have used the excitation wavenumber ν_0 = 9398.5 cm^{-1}, which corresponds to the wavelength of 1064 nm of a Nd:YAG laser), ν_i is the vibraional wavenumber of the i^{th} normal mode (cm^{-1}), while S_i is the Raman scattering activity of the normal mode ν_i, f (is a constant equal to 10^{-12}) is a suitably chosen common normalization factor for all peak intensities h, k, c and T are Planck and Boltzmann constants, speed of light and temperature in Kelvin, respectively.

4. Results and Discussion

4.1 Structural Properties

The labeling of atoms of the title compounds are shown in Fig. 1.The molecule contains F and NO2 group connected with benzene ring. The optimized values of bond lengths, bond angles and dihedral angles are reported in Table 1 calculated by B3LYP method with 6-311++G(d,p). Experimental and simulated spectra of FT-IR and FT-Raman are presented in Figs. 2 and 3, respectively. Normal coordinate analyses were carried out for the title compound to provide a complete assignment of fundamental frequencies. For this purpose, the full set of 54 standard internal coordinates (containing 12 redundancies) for DFDNB was defined as given in Table 2. From these, a non-redundant set of local symmetry coordinates were constructed by suitable linear combinations of internal coordinates following the recommendations of Fogarasi et al. [15, 16] are summarized in Table 3. The theoretically calculated force fields were transformed to this set of vibrational coordinates and used in all subsequent calculations.

The optimized molecular structure of DCNB reveals that the para-substituted nitro group is in planar with the benzene ring. Inclusion of the NO2 group and halogen F atoms known for its strong electron withdrawing nature in para position is expected to increase a contribution of the resonance structure, in which the electronic charge is concentrated at this site. The bond length between C–C of right moiety of the benzene ring is reduced where as the bond length of the left moiety is stretched out. Particularly the bond length stretching is greater at the place of NO2 group than F atom. It is also evident from the bond length order as C3–C4<C1–C6<C5–C6<C4–C5<C2–C3<C1–C2. The C–F bond length indicates a considerable increase when substituted in place of C–H. Therefore, the coherent of F atom at C which shares its π electron with the ring leads to some changes of the bond lengths and bond angles of the aromatic ring. The benzene ring appears to be a little distorted because of the NO2 group substitution as seen from the bond angles C3–C4–C5, which are calculated as 119.611◦ and 119.462◦, respectively, by B3LYP/6-311++G(d,p) method and are smaller than typical hexagonal angle of 120◦.

4.2 Vibrational Analysis

From the structural point of view, the title compound is assumed to have C1 point group symmetry. The 42 fundamental modes of vibrations arising for DFDNB are classified into 29A′ and 13A″ species. The A′ and A″ species represent the in-plane and out-of-plane vibrations, respectively. For visual comparison, the observed and calculated FT-IR and FT-Raman spectra of DFDNB at DFT/B3LYP level using 6-311++G(d,p) basis set are shown in Figs. 2 and 3, respectively. The detailed vibrational assignment of fundamental modes of DFDNB along with the calculated IR and Raman frequencies and normal mode descriptions (characterized by PED) are reported in Table 4. The calculated frequencies are scaled by 0.952 for in-plane bending and 0.945 for out-of-plane bending.

4.2.1. C–H vibrations

The nitro group does not appear to affect the position of characteristic C–H bands and these bands occur in the range 3100–3000 cm^{-1}. The in-plane C–H bending vibrations appear in the range 1300–1000 cm^{-1} in the substituted benzenes and the out-of-plane bending vibrations in the range 1000–750 cm^{-1} [21]. The FT-IR vibrational frequencies at 3300 and 3220 cm^{-1} are assigned to C–H stretching vibrations of DFDNB and show good agreement with the calculated results. The FT-Raman counter parts of C–H vibrations are observed at 2750 cm^{-1}, which are further supported by the PED contribution of almost 99%.

The FT-IR bands at 1300 $cm^{-1}$is assigned to C–H in-plane bending vibrations of title molecule. The calculated and observed frequencies assigned to two C–H out-of-plane bending vibrations are 600 cm^{-1} in FT-IR spectrum and 600 and 522 cm^{-1}in FT-Raman spectrum for DFDNB. The slight deviation in low frequency bands are due to the interaction between NO2 and C–H out-of-plane bending frequencies, which is also confirmed by PED output. The observed C–H out-of-plane bending modes show consistent agreement with the computed B3LYP results.

4.2.2. Nitro (NO2) group vibrations

For molecules with an NO2 group, the NO2 asymmetric stretching vibration band range is 1625–1540 cm^{-1} and that of the symmetric stretching vibration is 1400–1360 cm^{-1} [22]. The FT-IR bands observed at 1600 cm^{-1}in DFDNB with very strong intensity were within NO2 asymmetric stretching vibrations. The FT-Raman bands observed at 1480 and 1400 cm^{-1} and FT-IR bands at 1420 cm^{-1} were within NO2 symmetric stretching vibrations. Aromatic nitro compounds have a band of weak-to-medium intensity in the region 590–500 cm^{-1} [22] due to the in-plane deformation (scissoring and rocking) mode of the NO2 group. This was observed at 700 cm^{-1}in FT-IR spectrum. The deformation vibrations of NO2 group (rocking, wagging and twisting) contribute to several normal modes in the low frequency region [23]. The NO2 wagging vibrations is observed in the Raman spectrum at 318 cm^{-1} for DFDNB. As the torsion vibrations are very anharmonic, its frequency is difficult to reproduce within the harmonic approach.

4.2.3. C–C vibrations

The ring stretching vibrations are very much important in the spectrum of benzene and its derivatives are highly characteristic of the aromatic ring itself. The ring C–C and C–C stretching vibrations, known as semicircle stretching usually occur in the region 1400–1625 cm^{-1} [24]. Particularly, the bands between the regions 1590–1650 cm^{-1} [25] and 1590–1430 cm^{-1} [26] in benzene derivatives are usually assigned to C–C and the C–C stretching vibrations, respectively. In the present case, the C–C stretching vibrations are observed with weak and very strong intensity at 1250 cm^{-1} in FT-IR spectrum and 1220 cm^{-1} in FT-Raman spectrum. The calculated values are at 1324, 1289, 1125, 1014, 915 and 899 cm^{-1} by B3LYP method. It shows the theoretical values good agreement with experimental data. All the C–C stretching vibrations are observed well below the expected region. From this observation it is clear that the ring stretching vibrations are affected much due to the NO2 and F. In the present compound, the C–C–C out-of-plane bending vibrations is appeared weak intensity at 705 cm^{-1} in FT-Raman spectrum. All the assignments related to in-plane and out-of-plane bending vibrations are in coherent with the literature values [26].

4.2.4 C–N vibrations

In aromatic compounds, the C–N stretching vibration usually lies in the region 1400–1200 cm^{-1}. The identification of C–N stretching frequencies is a rather difficult task. Since the mixing of vibrations is possible in this region [25]. In this study, the bands observed at 1080 and 1050 cm^{-1} in FT-IR and 1003 cm^{-1} in FT-Raman spectra have been assigned to C–N stretching vibrations of DFDNB. The in-plane and out-of-plane bending C–N vibrations have also been identified and these assignments are also supported by the PED values.

4.2.5. C–F vibrations

Assignments of the C–F stretching modes are very difficult as these vibrations are strongly coupled with the other in-plane bending vibrations of several modes. The observed bands of the C–F stretching vibrations have been found to be very strong in the FT-IR spectra and these appear in the range 1000–1300 $cm^{-1}$for several fluoro-benzenes [27, 28]. And also the C–F stretching vibrations strongly coupled with the C–H in-plane bending vibrations in the mono fluorinated benzene and is observed in the region 1100–1000 cm^{-1} [29]. In the present case, the C–F stretching vibration is observed in FT-IR spectrum at 800 cm^{-1}.

The C–F in-plane-bending vibration mode for the mono fluorinated benzene is normally assigned at 250–350 cm^{-1} [30]. In the present case, the calculated C–F in-plane bending at 318 and 242 cm^{-1}. The predicted frequency of the C–F out-of-plane bending vibration assigned at 199 and 143 cm^{-1}. According to the reported values [31], this assignment is in line with the literature. All the C–F vibrations are found within the expected region which shows that these vibrations have not affected by other substitution in the ring.

5. NMR Spectral Analysis

The molecular structure of the title compounds is optimized. Then using gauge including atomic orbital (GIAO) ^{13}C NMR and ^{1}H NMR chemical shifts calculations of the title compounds were carried out using B3LYP method with 6-311++G(d,p) basis set. The GIAO method is one of the most common approaches for calculating isotropic nuclear magnetic shielding tensors. The NMR spectral calculations were performed using the Gaussian 09W program package. The experimental ^{13}C NMR and ^{1}H NMR spectra is shown in Fig. 4 for DFDNB.

Experimental and theoretical chemical shifts of DFDNB in ^{13}C NMR and ^{1}H NMR spectra were recorded and the obtained data are presented in Table 5. The linear correlations between calculated and experimental data of ^{13}C NMR and ^{1}H NMR spectra were noted. The protons are located on the periphery of the molecule and therefore are supposed to be more susceptible to molecular (solute-solvent) effects than carbons. For this reason, the agreement between the experimental and calculated data for protons is less than that of carbon-13 [32]. The range of the ^{13}C NMR

chemical shifts for a typical organic molecule usually is >100 ppm and the accuracy ensures reliable interpretation of spectroscopic parameters. In the present study, the ^{13}C NMR chemical shifts in the ring for DFDNB is >100 ppm, as expected.

6. Thermodynamic Properties

Several thermodynamic properties like heat capacity, zero pointenergy, entropy along with the global minimum energy of DFDNB have been obtained by density functional method using 6-311++G(d,p) basis set calculations are presented in Table 6. The difference in the values calculated by both the methods is only marginal. Scale factors have been recommended [33] for an accurate prediction in determining the zero-point vibration energy (ZPVE), and the entropy (Svib). The variation in the ZPVE seems to be insignificant. The total energy and the change in the total entropy of DFDNB at room temperature are also presented.

7. Conclusion

FT-IR and FT-Raman spectra of DFDNB were recorded and the detailed vibrational assignments were obtained. The molecular geometry,vibrational frequencies, infrared intensities and Raman scattering activities of the molecules were calculated by DFT (B3LYP) method with 6-311++G(d,p) basis set. ^{1}H and ^{13}C NMR chemical shifts were compared with experimental values. As a result, all the vibrational frequencies were calculated and scaled values were compared with experimental FT-IR and FT-Raman spectra. The observed and the calculated frequencies are in good agreement. The difference between the corresponding wavenumbers (observed and calculated) is very small for most of fundamentals. Therefore, the results presented in this work for DFDNB indicate that this method is reliable for prediction of both FT-IR and FT-Raman spectra of the title compounds. NMR chemical shifts wavelengths have been found to be in a good agreement with experimental values.

References

[1] T. Bezrodna, G. Puchkovska, V. Shimanovska, T. Gavrilko, Journal of Molecular Structure 2002; 615: 89–96.
[2] H. Ratinen, M. Kiviharju, Spectrochimica Acta Part A 1989; 45: 729–734.
[3] W. Domalewski, L. Stefaniak, G.A. Webb, Journal of Molecular Structure 1993; 295: 19–23.
[4] M.A. Palafox, F.J. Melendez, Journal of Molecular Structure (Theochem) 2003; 625: 17–21.
[5] Q.G. Huang, L.R. Kong, Y.B. Liu, L.S. Wang, Relationships Between Molecular Structure and Chromosomal Aberrations in Vitro Human Lymphocytes Inducedby Substituted Nitrobenzene, 1996.
[6] V. Mukherjee, N.P. Singh, R.A. Yadav, Spectrochimica Acta Part A 2010; 77: 787–794.
[7] W. Lewandowski, M. Kalinowska, H. Lewandowska, Inorganica Chimica Acta 2005; 358: 2155–2166.
[8] M. Karabacak, M. Cinar, A. Coruh, M. Kurt, Journal of Molecular Structure 2009; 919: 26–33.
[9] I.F. Shishkov, L.V. Khristenko, L.V. Vilkov, S. Samdal, S. Gundersen, Structural Chemistry 2003; 14(2): 151–157.
[10] M.J. Frisch et al., Gaussion 09 Program, Gaussian, Inc., Wallingford, CT, 2004.
[11] A.D. Becke, Journal of Chemical Physics 1993; 98: 5648–5652.
[12] C. Lee, W. Yang, R.G. Parr, Physics Review B 1998; 37: 785–789.
[13] P. Pulay, G. Fogarasi, G. Pongor, J.E. Boggs, A. Vargha, Journal of American Chemical Society 1983; 105: 7037–7047.
[14] G. Rauhut, P. Pulay, Journal of Physical Chemistry 1995; 99: 3093–3100.
[15] G. Fogarasi, P. Pulay, in: J.R. Durig (Ed.), Vibrational Spectra and Structure (Chapter3), Elsevier, Amsterdam, 1985; 14: 125–130.
[16] G. Fogarasi, X. Zhou, P.W. Taylor, P. Pulay, Journal of American Chemical Society 1992; 114:8191–8201.
[17] T. Sundius, Journal of Molecular Structure 1990; 218: 321–326.
[18] (a) T. Sundius, Vibirational Spectroscopy 2002; 29: 89–95;
(b) Molvib (V.7.0): Calculation of Harmonic Force Fields and Vibrational Modes of Molecules, QCPE Program No. 807, 2002.
[19] G. Keresztury, J.M. Chalmers, P.R. Griffiths (Eds.), Raman Spectroscopy: Theory in Hand Book of Vibrational Spectroscopy, John Wiley & Sons Ltd., New York, 2002; 1.
[20] G. Keresztury, S. Holly, G. Besenyei, J. Varga, A.Y. Wang, J.R. Durig, Spectrochimica Acta Part A 1993; 49: 2007–2026.
[21] V. Krishnakumar, N. Prabavathi, Spectrochimica Acta Part A 2009; 72: 738–742.
[22] G. Socrates, Infrared and Raman Characteristic Group Frequencies–Tables and Charts, 3rd edition, John Wiley & Sons, Chichester, 2001.
[23] E. Gladis Anitha, S. Joseph Vedhagiri, K. Parimala, Spectrochimica Acta Part A 2015; 136:1557–1568.
[24] G. Varsanyi, Vibrational Spectra of Benzene Derivatives, Academic Press, New York, 1969.
[25] D.N. Sathyanarayana, Vibrational Spectroscopy Theory and Application, New Age International Publishers, New Delhi, 2004.
[26] S.P. Saravanan, A. Sankar, K. Parimala, Journal of Molecular Structural 2017; 1127: 784–195.
[27] V.J. Eatch, D. Steel, Journal of Molecular Spectroscopy 1973; 48: 446–449.
[28] M.P. Kumpawat, A. Ojha, N.D. Patel, Canadian Journal of Spectroscopy 1980; 25:1–12.
[29] I.L. Tocon, M. Becucci, G. Pietraperzia, E. Castellucci, J.C. Otero, Journal of Molecular Structure 2001; 565: 421–425.
[30] M.S. Navti, M.A. Shashidar, Indian Journal of Physics 1994; 668: 371–373.
[31] N. Sundaraganesan, C. Meganathan, B.D. Joshua, P. Mani, A. Jayaprakash, Spectrochimica Acta Part A 2008; 71: 1134–1139.
[32] B. Osmialoswski, E. Kolehmainen, R. Gawinecki, Magnetic Resonance Chemistry 2001; 39: 334–340.

[33] J. Annama, P. Daizy, K.I. Abdullah, G. Keresztury, S. Devanarayanar, Journal of Raman Spectroscopy 2000; 31: 1067–1071.

Table 1: Bond lengths (Å), bond angles (°) and dihedral angles (°) for DFDNB calculated by B3LYP/6-311 ++G(d,p) method

Bond lengths	Values (Å)	Bond angles	Values (°)	Dihedral angles	Values(°)
C1–C2	1.386	C2–C1–C6	120.487	C6–C1–C2–C3	–1.317
C1–C6	1.403	C2–C1–F7	117.829	C6–C1–C2–N8	178.241
C1–F7	1.327	C6–C1–F7	121.649	F7–C1–C2–C3	–179.241
C2–C3	1.387	C1–C2–C3	119.462	F7–C1–C2–N8	0.318
C2–N8	1.082	C1–C2–N8	120.258	C2–C1–C6–C5	–0.311
C3–C4	1.405	C3–C2–N8	120.279	C2–C1–C6–H16	179.326
C3–H11	1.428	C2–C3–C4	120.486	F7–C1–C6–C5	177.531
C4–C5	1.388	C2–C3–H11	117.854	F7–C1–C6–H16	–2.831
C4–N12	1.477	C4–C3–H11	121.626	C1–C2–C3–C4	1.316
C5–C6	1.389	C3–C4–C5	119.611	C1–C2–C3–H11	179.234
C5–F15	1.082	C3–C4–N12	122.304	N8–C2–C3–C4	–178.242
C6–H16	1.476	C5–C4–N12	118.084	N8–C2–C3–H11	–0.324
N8–O9	1.219	C4–C5–C6	120.306	C1–C2–C3–C4	0.313
N8–O10	1.222	C4–C5–F15	119.853	C2–C3–C4–N12	–179.319
N12–O13	1.223	C6–C5–F15	119.841	H11–C3–C4–C5	–177.525
N12–O14	1.225	C1–C6–C5	119.606	H11–C3–C4–N12	2.843
		C1–C6–H16	122.317	C3–C4–C5–C6	–1.962
		C5–C6–H16	117.476	C3–C4–C5–F15	178.083
		C2–N8–O9	118.076	N12–C4–C5–C6	177.686
		C2–N8–O10	116.678	N12–C4–C5–F15	–2.269
		O9–N8–O10	125.836	C3–C4–N12–O13	25.734
		C4–N12–O13	116.687	C3–C4–N12–O14	–155.366
		C4–N12–O14	117.493	C5–C4–N12–O13	–153.904
		O13–N12–O14	125.811	C5–C4–N12–O14	24.996
				C4–C5–C6–C1	1.961
				C4–C5–C6–H16	–177.692
				F15–C5–C6–C1	–178.084
				F15–C5–C6–H16	2.263
				C1–C2–N8–O9	155.391
				C1–C2–N8–O10	–25.700

Table 2: Definition of internal coordinates for DFDNB

No (i)	Symbol	Type	Definition
Stretching			
1–6	P_i	C⍰C	C1–C2, C2–C3, C3–C4, C4–C5, C5–C6, C6–C1
7–8	q_i	C⍰H	C3–H11, C6–H16
9–10	D_i	C⍰F	C1–F7, C5–F15
11–12	Q_i	C⍰N	C2–N8, C4–N12
13–16	r_i	N⍰O	N8–O9, N8–O10, N12–O13, N12–O14
Bending			
17–22	α_i	C⍰C⍰C	C1–C2–C3, C2–C3–C4, C3–C4–C5, C4–C5–C6, C5–C6–C1, C6–C1–C2
23–26	Bi	C⍰C⍰H	C1–C6–H16, C5–C6–H16, C4–C3–H11, C2–C3–H11
27–30	ψ_i	C⍰C⍰F	C2–C1–F7, C6–C1–F7, C4–C5–F15, C6–C5–F15
31–34	Φi	C⍰C⍰N	C1–C2–N8, C3–C2–N8, C3–C4–N12, C5–C4–N12
35–38	γ_i	C–N–O	C2–N8–O9, C2–N8–O10, C4–N12–O13, C4–N12–O14
39–40	Σi	O–N–O	O9–N8–O10, O13–N12–O14
Out-of-plane bending			
41–42	ω_i	C⍰C⍰C–H	H11–C3–C4–C2, H16–C6–C1–C5
43–44	ω_i	C⍰C⍰C⍰F	F7–C1–C6–C2, F15–C5–C4–C6
45–46	ψ i	C⍰C⍰C⍰N	N8–C2–C1–C3, N12–C4–C3–C5
Torsion			
47–52	τ_i	τRing	C1–C2–C3–C4, C2–C3–C4–C5, C3–C4–C5–C6, C4–C5–C6–C1, C5–C6–C1–C2, C6–C1–C2–C3
53–54	τ_i	τNO2	C2–N8–O9–O10, C4–N12–O13–O14

Table 3: Definition of local symmetry coordinates for DFDNB.

No(i)	Symbol	Definition
1–6	νCC	P1, P2, P3, P4, P5, P6
7–8	νCH	q7, q8
9–10	νCF	D9, D10
11–12	νCN	Q11, Q12
13–14	NO2sym	(r13+r14)/√2, (r15+r16)/√2
15–16	NO2asym	(r13–r14)/√2, (r15–r16)/√2
17	Rtrigd	(α17–α18+α19–α20+α21–α22)/√6
18	Rsymd	(–α17–α18+2α19–α20–α21+2α22)/√12
19	Rasymd	(α19–α20+α21–α22)/√2
20–21	bCH	(β23–β24)/√2, (β25–β26)/√2
22–23	bCF	(ψ27–ψ28)/√2, (ψ29–ψ30)/√2
24–25	bCN	(υ31–υ32)/√2, (υ33–υ34)/√2
26–27	NO_2 twist	(γ35+γ36)/√2, (γ37+γ38)/√2
28–29	NO_2 rock	(γ35–γ36)/√2, (γ37–γ38)/√2
30–31	NO_2sciss	(σ39–γ35–γ36)/√2, (σ40–γ37–γ38)/√2
32–33	γCCH	ω41, ω42
34–35	γCCF	ω43, ω44
36–37	γCCN	ψ45, ψ46
38	tRtrigd	(τ47+τ48+τ49+τ50+τ51+τ52)/√6
39	tRsymd	(τ47+τ49+τ50+τ52)/2
40	tRasymd	(–τ47+2τ48–τ49–τ50+2τ51–τ52)/√12
41–42	NO2wagg	τ53, τ54

Table 4: Observed and B3LYP/6-311++G(d,p) level calculated vibrational frequency (cm^{-1}), IR Intensity (Km mol^{-1}), Raman intensity ($Å^4amu^{-1}$), Reduced masses (amu), force constants (m dyne $Å^{-1}$), depolarization ratios are obtained for DFDNB.

No.	Observed wavenumbers (cm^{-1})		Calculated wavenumbers (cm^{-1})		IR intensity	Raman intensity	Reduced mass	Force constant	Depolar (P)	Depolar (U)	[a]PED (%) among type of internal coordinates
	FT-IR	FT-Raman	Unscaled	Scaled							
1	3300(w)		3226	2992	23.55	42.09	1.09	6.69	0.17	0.29	νCH(99)
2	3220(vw)	2750(vw)	3218	2816	9.48	100.12	8.28	6.66	0.25	0.41	νCH(99)
3	1600(vs)		1662	1545	289.58	37.08	1.09	13.49	0.75	0.85	NO2asym(89)
4			1644	1487	370.04	4.63	11.89	18.95	0.21	0.35	NO2asym(87)
5			1598	1324	66.62	32.28	12.85	19.35	0.71	0.83	νCC(84)
6			1594	1289	139.36	46.63	12.70	19.03	0.56	0.72	νCC(82)
7		1480(vw)	1513	1214	72.03	4.97	3.89	5.25	0.74	0.85	NO2sym(80)
8	1420(s)	1400(vw)	1444	1182	7.12	3.50	11.02	13.55	0.44	0.62	NO2sym(78)
9			1375	1125	112.82	89.20	14.02	15.64	0.13	0.23	νCC(71)
10			1369	1014	274.41	22.97	12.37	13.66	0.71	0.83	νCC(65)
11	1300(s)		1351	985	133.56	27.87	12.16	13.09	0.74	0.85	βCH(63), Rtrigd(41)
12			1310	964	181.13	75.44	10.76	10.89	0.10	0.18	βCH(58), Rsymd(32)
13	1250(w)	1220(vs)	1235	915	4.97	0.01	1.37	1.23	0.75	0.85	νCC(54)
14			1181	899	56.37	3.32	2.02	1.66	0.74	0.85	νCC(49)
15	1080(m)		1153	872	0.24	22.30	10.04	7.87	0.18	0.31	νCN(58), βCH(32)
16	1050(m)	1003(vw)	1060	863	122.51	2.81	3.05	2.02	0.74	0.85	νCN(51), βCF(29)
17			953	852	22.49	0.16	1.41	0.76	0.43	0.60	νCF(46), νCN(27), βCH(22)
18			879	847	13.96	2.57	6.52	2.97	0.75	0.85	Rtrigd(46),νCH(29), νCF(14)
19			862	809	25.88	0.47	1.49	0.65	0.43	0.60	Rasymd(40),βCN(13),νCF(11)
20	800(w)		851	724	22.24	16.49	13.49	5.76	0.04	0.08	νCF(38), Rtrigd(21), βCH(18)
21			784	705	1.52	0.99	12.56	4.55	0.75	0.85	NO2 sciss(65)
22			752	685	6.47	7.76	8.27	2.76	0.11	0.20	NO2 sciss(58)
23	700(w)		747	665	10.79	6.66	6.33	2.08	0.09	0.17	NO2 rock(48)
24		705(w)	719	623	45.76	1.33	8.68	2.64	0.75	0.85	Rsymd(39), βCF(24),νCN(15)
25			662	589	2.01	0.88	4.43	1.15	0.74	0.85	NO2 rock(42)
26			651	572	14.36	0.87	7.54	1.88	0.75	0.85	tRtrigd(36),γCH(14), γCF(12)
27		600(w)	621	514	0.29	1.21	7.96	1.81	0.75	0.85	γCH(31),tRtrigD(31), γCF(12)
28	600(s)	522(vw)	601	599	19.04	2.63	9.49	2.02	0.72	0.83	γCH(33), tRtrigD(24)
29			205	387	0.52	3.26	6.23	0.92	0.16	0.27	tRasym(39),γCF(38)
30			454	353	1.58	1.32	4.42	0.53	0.65	0.79	tRsymd(29),γCF(26),γCN(11)
31			435	318	1.20	0.06	13.30	1.48	0.74	0.85	βCF(28), Rsymd(36),βCH(12)
32			362	309	1.84	4.64	13.83	1.07	0.30	0.46	βCN(27),νCF(36),βCH(12)
33		318(vw)	333	298	0.04	1.25	13.54	0.88	0.75	0.85	NO2 wagg(44), γCN(20)
34			311	278	2.25	2.03	16.61	0.94	0.06	0.12	βCN(37), βCH(36),νCF(12)
35			309	242	0.60	1.51	13.87	0.78	0.74	0.85	NO2 wagg(34), βCN(20)
36			242	214	0.47	1.83	7.30	0.25	0.74	0.85	βCF(27),νCC(36),βCN(12)

37			238	199	0.95	0.44	14.36	0.48	0.75	0.85	γCF(20), Rsymd(17),νCN(13)
38			157	143	2.39	0.52	14.34	0.21	0.59	0.74	γCF(46), tRsymd(18), γCH(15)
39			132	118	8.46	0.55	9.62	0.09	0.67	0.80	γCN(36),tRasymd(18),γCH(15)
40			80	43	0.00	0.08	17.35	0.06	0.75	0.85	γCN(31), tRsymd(18), γCF(15)
41			44	35	0.55	2.52	15.46	0.05	0.73	0.84	NO2 twist(38)
42			39	27	0.21	0.78	15.86	0.01	0.74	0.85	NO2 twist(23)

Raman intensities calculated by Equation 2 and normalized to 100.[a]Only contributions larger than 10% are given.

Experimental relative intensities are abbreviated as follows: vs-very strong, s-strong, m-medium, w-weak, vw-very weak. Abbreviations; ν-stretching, sym-symmetric stretching, asym-asymmetric stretching, b-bending, d-deformation, R-ring, sciss-scissoring, rock- rocking, wagg-wagging, twist-twisting, β- in-plane bending, γ- out-of-plane bending, t-torsion, trig-trigonal.

Table 5: The experimental and calculated ^{13}C and ^{1}H NMR isotropic chemical shifts (δ in ppm) of DFDNB by B3LYP/6-311++G(d,p) level of theory

Atoms	Experimental	Theoretical
C1	115	114.15
C2	125	131.94
C3	118	118.49
C4	134	141.67
C5	159	155.15
C6	162	157.06
H11	9	7.96
H16	7.5	7.54

Table 6: The calculated thermodynamics and molecular parameters are for DFDNB.

Parameters	Values
Rotational Temperature (Kelvin)	0.056
	0.238
	0.017
Rotational countant (GHZ)	1.174
	0.495
	0.355
Zero Point vibrational energy (Jules / Mol)	231310.6 (Joules / Mol) 55.2845 (Kcal / Mol)
Vibrational Temperature (Kelvin)	1970.07
	56.22 64.21 115.11 190.23 226.91 342.97 348.35 444.73 447.54 479.44 521.30 627.04 654.56 722.56 865.61 893.66 937.56 1034.99 1075.04 1082.47 1225.15 1240.44 1265.72 1371.71 1526.10 1660.16 1699.85 1778.16 1886.07 1944.62 1970.07

Zero Point Correction (Hartree/Particle)	0.0881
Thermal Correction to Energy	0.0993
Thermal Correction to Enthalpy	0.1003
Thermal Correction to Gibbs free energy	0.0491
Sum of electronic and Zero Point Energies	–839.8537
Sum of electronic and thermal energies	–839.8424
Sum of electronic and thermal Enthalpies	–839.8415
Sum of electronic and thermal Free Energies	–839.8927

Figure captions

Figure 1: Molecular model of DFDNB along with numbering of atoms.

Figure 2: Comparison of observed and calculated FT-IR spectra of DFDNB: (a) observed; (b) calculated with B3LYP/6-311++G(d,p).

Figure 3: Comparison of observed and calculated FT-Raman spectra of DFDNB: (a) observed; (b) calculated with B3LYP/6-311++G(d,p).

Figure 4: Experimental NMR spectrum of DFDNB: (a) ^{13}C and (b) ^{1}H.

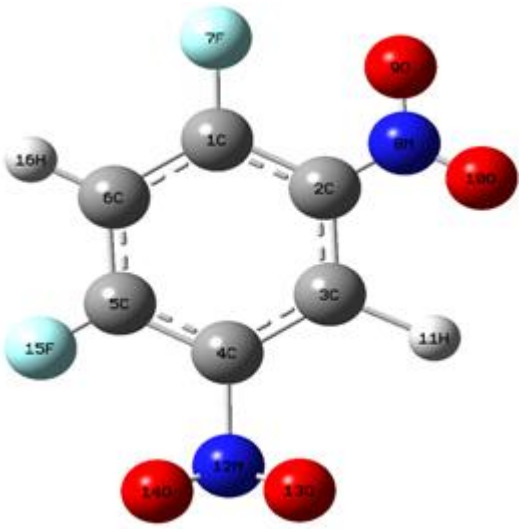

Figure 1

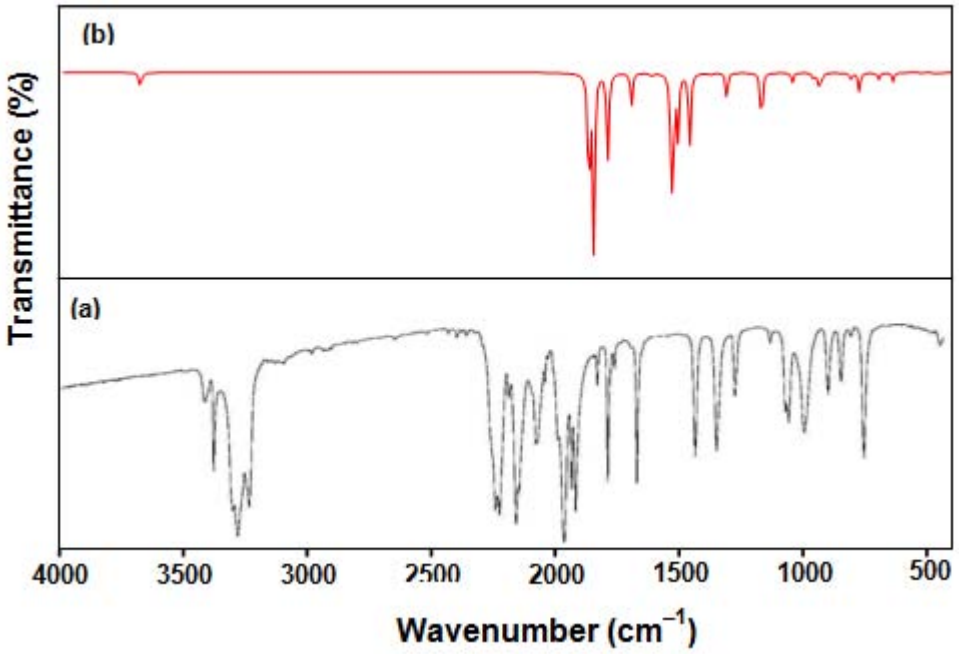

Figure 2

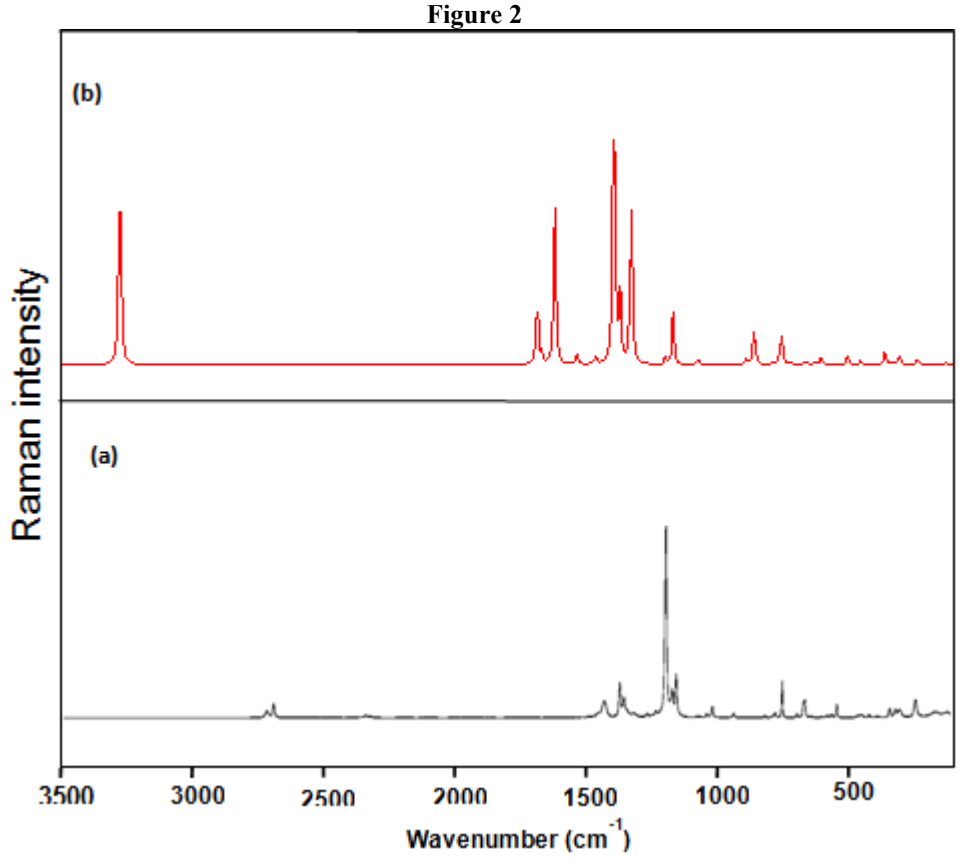

Figure 3

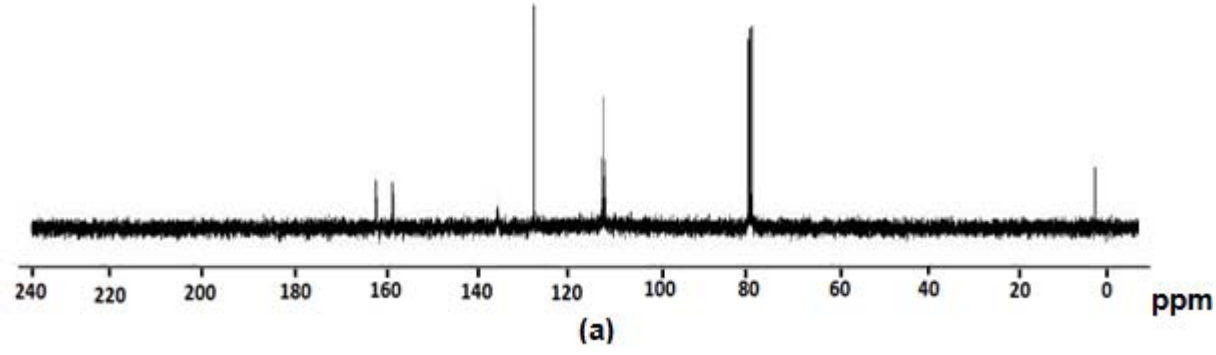

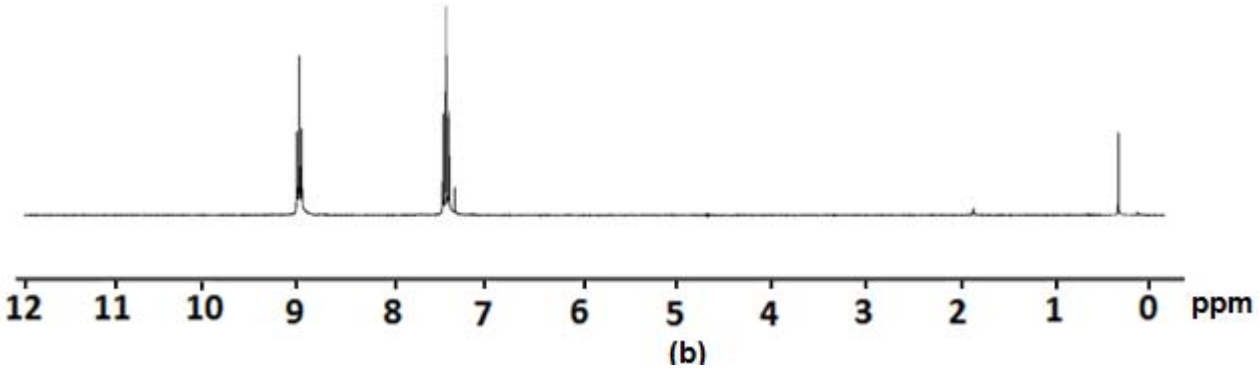

(b)

Figure 4